Thermally-Activated Delayed Fluorescence Mediated Through the Upper Triplet State Manifold in non-Charge Transfer Star-Shaped Triphenylamine-Carbazole Molecules

Piotr Pander,[†] Radoslaw Motyka,[‡] Pawel Zassowski,[‡] Marc K. Etherington,[†] Daniele Varsano,[§] Tales J. da Silva,[‖] Marilia J. Caldas,[‖] Przemyslaw Data,[†,‡,⊥] and Andrew P. Monkman [†]*

[†] Department of Physics, Durham University, South Road, Durham, DH1 3LE, United Kingdom.

[‡] Faculty of Chemistry, Silesian University of Technology, Ks. M. Strzody 9, 44-100 Gliwice, Poland

[§] S3 Center, CNR Institute of Nanoscience, Modena, Italy

[‖] Institute of Physics, University of São Paulo, São Paulo, Brazil

[⊥] Centre of Polymer and Carbon Materials, Polish Academy of Sciences, M. Curie-Sklodowskiej 34, 41-819 Zabrze, Poland

AUTHOR INFORMATION

Corresponding Author

Dr. Przemyslaw Data, e-mail: Przemyslaw.Data@durham.ac.uk

ABSTRACT

Thermally-activated delayed fluorescence has been found in a group of tricarbazolylamines which are purely electron-donating, non-charge transfer (CT) molecules. We show that the reverse intersystem crossing step in these materials is mediated through upper triplet states. Reverse internal conversion is shown to be the thermally-activated mechanism behind the triplet harvesting mechanism. The strongly mixed n-π*/π-π* character of the lowest energy optical transitions retains high oscillator strength and gives rise to high Φ_{PL}. OLED devices using these materials were fabricated to show very narrow (FWHM = 38 to 41 nm) electroluminescence spectra, clearly demonstrating the excitonic nature of the excited states. This new combination of physicochemical properties of a non-CT molecule yield TADF, but via a different, physical mechanism, reverse internal conversion delayed fluorescence (rICDF*)*.

INTRODUCTION

Since the introduction of thermally-activated delayed fluorescence (TADF) emitters in organic light-emitting diodes (OLEDs)[1] a wide variety of TADF molecules have been described in the literature.[2–8] Doping TADF molecules into a host is seen to be the most promising route to form an emissive layer in a device, due to the high external quantum efficiencies (EQEs) that have been achieved.[5–7] There is also the possibility of utilizing exciplex states, either as the emissive state or to enhance low energy emitters.[9–12] Recently, polymers and small molecules that exhibit aggregation-induced emission have been found to display TADF, and while their device performance is currently low, they demonstrate the concept of using the pure compound without a host.[13–15]

Here, we describe a type of molecule that exhibits a TADF phenomenon without having charge transfer excited states. Because of this, these non-CT TADF emitters can exhibit relatively narrow or structured emission spectrum compared to the broad Gaussian bands from TADF emitters having CT excited states. This feature makes them far more useful in OLED display applications. There have been several reports in the literature of non-CT based TADF, but none provide an adequate description of the possible mechanism giving rise to the TADF component. Hatakeyama *et al.* [16] have published a material based on nitrogen-boron that they report demonstartes a multiple resonance effect, decoupling HOMO and LUMO, that shows a non-charge transfer mediated DF and which they report as exhibiting TADF and excellent device performance. However, the authors show no data to explain what mechanism gives rise to TADF in this material. Although the reported EQE is excellent (20.2 %), the maximum brightness achieved is very low with rapid performance roll-off. Li *et al*. have reported an acceptor-based planar molecule that exhibits a thermally activated delayed emission and OLEDs yielding EQEs

of 6%.[17] Also, through excited state proton transfer, Mamada *et al.* have demonstrated TADF analogous to that found in intramolecular charge transfer (ICT) in molecules that are not themselves CT.[18]

The key to understanding TADF in ICT molecules is a very small HOMO – LUMO overlap which gives rise to minimal electron exchange energy and a very small energy gap between the singlet and triplet energy levels of the charge-transfer state, of order <0.05 eV.[2–7] The use of the resonant effect[16] is one important way to separate the HOMO and LUMO in a TADF emitter, but this still requires the presence of distinct electron-donating and electron-accepting atoms in the structure. However, as theoretically predicted by Lim *et al.* [19] and experimentally shown by Dias *et al.*,[20] in the case of CT states, spin-orbit coupling (SOC) between the singlet and triplet CT state is forbidden, and it is necessary to have a third, different state very close in energy to S_1 and T_1 to mediate SOC and enable the reverse intersystem crossing (rISC) step.[21,22] Thus, in ICT molecules TADF occurs by a second order vibronic and spin coupling mechanism, with a locally excited triplet state (^{3}LE) of the donor or acceptor unit acting as the mediator state. Li *et al*.[17] reported a moderate HOMO – LUMO overlap in their heptazine derivative that can be achieved without D-A structure. However, the molecule reported by Li *et al*. was planar, and no mechanism for the TADF process was given. Instead, they euphemistically called it a "hidden, efficient TADF pathway", but it may bare a similarity to the later reported nitrogen-boron systems using a multiple resonance effect.[16]

In this work, a new series of donor-type non-CT thermally-activated emitters are described (**Figure 1a**). These triphenylamine-carbazoles are non-planar and propeller-shaped and show thermally activated delayed emission behavior, different to typical CT TADF materials. The molecule **TCA_C4** gives sky-blue electroluminescence. This emission corresponds to that called

Bio-Blue OLEDs, introduced by Samsung, to reduce blue light stress to eyes relative to the current LCD and AMOLED displays.[23] Surprisingly, a similar molecule to the ones presented in this work has previously been reported, but TADF was not observed.[24] Using these materials we demonstrate that TADF arises through the mechanism of reverse internal conversion, hence reverse internal conversion delayed fluorescence 'rICDF' (**Figure 1 b**). For this mechanism to be efficient we show that that the lowest triplet states of the molecule are closely spaced and in **TCA_C4** T_2 and T_3 are very close in energy to S_1 facilitating efficient rISC. We postulate that reverse internal conversion between the triplet states gives rise to the upper triplet state population at room temperature and thus efficient rISC to S_1.

RESULTS AND DISCUSSION

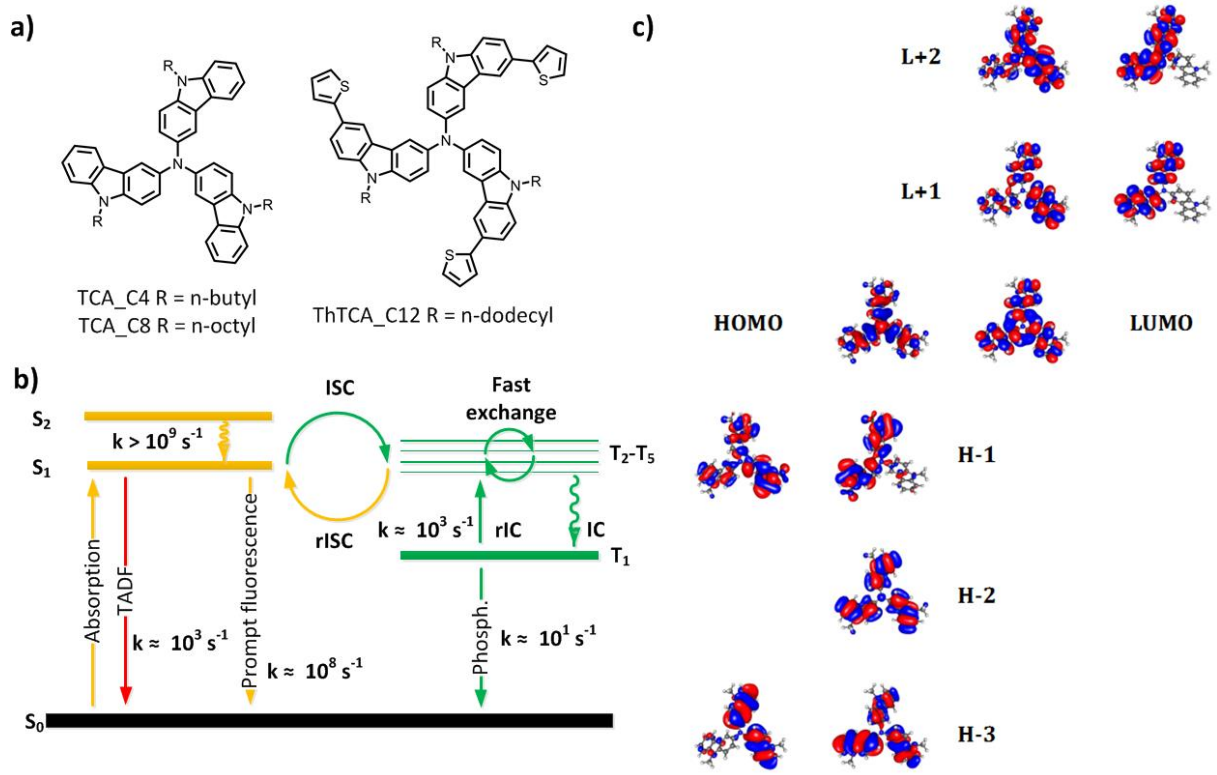

Figure 1. a) Materials studied in this work. b) Energy diagram showing the thermally activated delayed fluorescence (TADF) process between singlet and triplet excited states driven by reverse internal conversion (rIC) in **TCA_C4**, rICDF. c) Kohn-Sham orbital density isosurfaces of **TCA** core for the states close to the HOMO-LUMO gap; degenerate states are shown side-by-side. Results from computation through Gaussian09, cc-pVTZ basis set.

Details of the synthetic procedures and characterisation of the materials are given in full in the supplementary information (sections 1 and 2 in the SI). In **TCA_C4** the absorption bands (**Figure 2a**) below 350 nm (λ_{max} = 242, 289, 321 nm) can be attributed to π-π^* transitions while those at lower energy (λ_{max} = 375, 410 nm) to mixed $n\pi^*$-$\pi\pi^*$ transitions due to their lower molar absorption coefficients, but they are clearly not forbidden transitions (**Table S1**), Excitation into any of these bands results in emission from the same state, **Figure S1**. The two energetically

lowest absorption bands show weak, negative solvatochromism in accordance with our identification and the strong nπ* contribution to the mixed transitions (**Figure S2**). Importantly, the Φ_{PL} of **TCA_C4** is high (0.62), which is consistent with relatively large absorption coefficients (for the n-π^*/π-π* transition), thus suggesting high oscillator strength of the HOMO-LUMO transition given by the strongly mixed character of the transitions (**Table S2**).

Analysis of the absorption spectrum of the molecule **ThTCA_C12** in light of **TCA_C4** leads to similar conclusions. Absorption bands below 360 nm (λ_{max} = 245, 295, 334 nm) are attributed to π-π^* transitions while the 400-450 nm band can be attributed to a mixed n-π^* transition (**Figure S18**). The thiophene units present in **ThTCA_C12** have insignificant influence on the electronic structure of the molecule, however, the fluorescence spectrum in cyclohexane of this molecule is slightly red-shifted (λ_{max} = 459 nm for **TCA_C4** and λ_{max} = 465 nm for **ThTCA_C12**, see **Figure 2 a** and **Figure S18**).

Both materials have a moderate ΔE_{ST} gap in zeonex (0.21 eV in **TCA_C4** and 0.28 eV in **ThTCA_C12**), see **Figure 2 d** and **Figure S19 b**. Incorporation of the thiophene units not only slightly red-shifts the emission but also moderately widens the singlet-triplet gap (ΔE_{ST}), showing that the thiophene unit has more effect on the lowest energy triplet state of the molecule.

The non-planar structure and presence of non-bonding electrons are the key factors to achieving a moderate $\Delta E_{S\text{-}T}$ of order 0.2 eV, in the case of **TCA_C4** and **ThTCA_C12** (**Figure 1 c**, also see calculations in section 7 of the SI). In **TCA_C4** and **ThTCA_C12** the HOMO is a mixed *n-π* state, with the lone pairs coming from the nitrogen atoms of the central triphenylamine unit. This mixing gives stronger ground state coupling to the excited states as seen by the order of magnitude higher extinction coefficients and far higher photoluminescence

quantum yields (SI **Table S2**) from our materials as compared to those of Li *et al.* [17] The LUMO is distributed among the aromatic backbone of the molecule (see **Figure 1 c**), which again suggests that the excited states have a mixed ($n\pi^*+\pi\pi^*$) character (see also calculations in section 7 of the SI). The HOMO and LUMO wave functions are located almost in anti-phase, **Figure 1 c**. Considering these calculations, the S_1 state is mixed ($^1n\pi^*+^1\pi\pi^*$) in both molecules, whereas the lowest triplet state T_1 may be attributed to ($^3n\pi^*+^3\pi\pi^*$), with both showing the same orbital geometry.

In this work, TCA (**TCA_C4**, **TCA_C8**) was prepared with two different alkyl chains (C4, C8) and in both cases, the same properties were found (see section 6 of the SI for details). There is no effect from the alkyl chain in **TCA**. Surprisingly the **TCA_C4** and **ThTCA_C12** molecules have identical HOMO-LUMO distribution, probably because the thiophene ring is only moderately electron-donating while the rest of the molecule has strong electron-donating properties, so that the thiophene ring in **ThTCA_C12** contributes very little to the frontier orbital electronic structure of the molecule. Having established this, all effects are attributed to the core and as such this work will focus on **TCA_C4**.

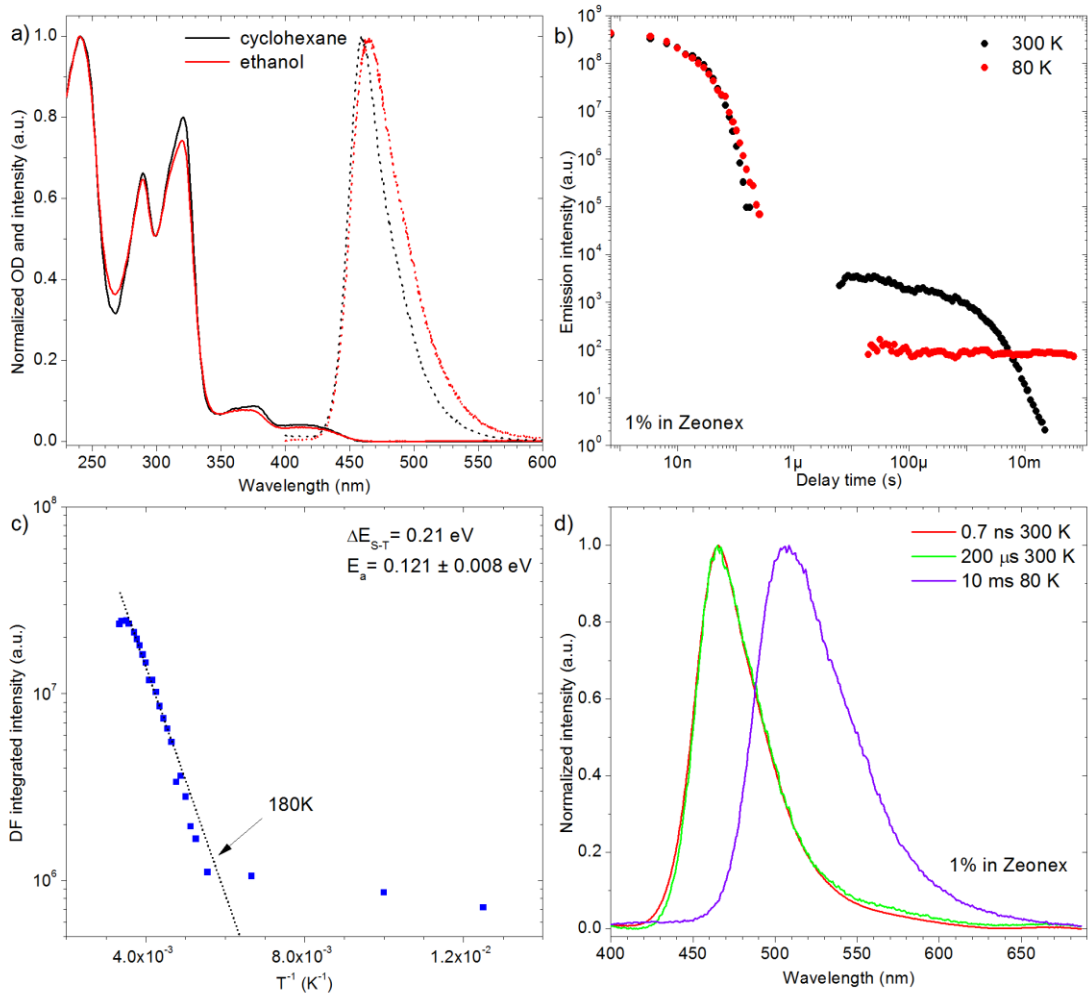

Figure 2. a) Emission and absorption spectra of **TCA_C4** in a polar and non-polar solvent at 10^{-5} M concentration; b) - photoluminescence decay transients observed at different temperature in a zeonex film of 1% **TCA_C4**; c) - temperature dependence of delayed fluorescence in a zeonex film of 1% **TCA_C4**; d) Time-resolved spectra showing prompt and delayed fluorescence and phosphorescence of 1% **TCA_C4** in a zeonex film.

The absorption and emission spectra of **TCA_C4** (**Figure 2a**) show that the polarity of the solvent has almost no impact on the photophysical behavior of the molecule with no shift in fluorescence onset apparent between cyclohexane (ε = 2.0) and ethanol (ε = 24.5). This clearly shows that there is no charge transfer (CT) character to the excited S_1 state and the observed

fluorescence emission originates from a local mixed ($^1n\pi^*+^1\pi\pi^*$) state. However, the small change in the shape of the emission spectrum in ethanol is ascribed to hydrogen bonding interactions between the lone pair on the nitrogen atoms and a hydroxyl group from ethanol. This effect confirms that the non-bonding electron pair of the nitrogen is involved in the singlet excited state. Further, the low energy absorption bands can be quenched on acidification of the **TCA_C4, Figure S3.** Because these are strongly mixed states, not pure $n\pi^*$ states, the PLQY remains very high, 0.62 in toluene and up to 0.89 in zeonex with an excited state lifetime of 17.6 ns (SI **Table S2**, **Figure S4-S5**), giving a radiative decay rate, k_{rad} of 3.5×10^7 s^{-1}.

Oxygen quenching of the photoluminescence of **TCA_C4** in solution and film was analysed to quantitively determine the contribution of DF to the total emission (**Figures S4-S6**, **Figure S7 c**,**d**, **Figure S8 c**,**d**), as oxygen quenches triplet states. It was observed that the DF in the solid state is strongly quenched by the presence of oxygen (**Figure S7 c**,**d**, **Figure S8 c**,**d**), confirming its triplet origin. In the solid state, the prompt fluorescence is not affected by oxygen due to the limited oxygen diffusion rate compared to the fast prompt radiative decay rate. We observed significant oxygen-quenching, greater than in zeonex or mCP, in toluene solution (**Figures S4-S6**). Most importantly, removal of oxygen increases the fluorescence intensity by *ca.* 2.4 times and increases the prompt fluorescence lifetime from 7.3 ns in air-equilibrated solution to 17.6 ns in a degassed solution. This is consistent with similar singlet fluorescence quenching in molecules like diphenylanthracene or other aromatic hydrocarbons.[25–27] In **TCA_C4** a large oxygen quenching effect can be observed, although no long-lived delayed fluorescence is observed in solution, **Figure S9**, the non-radiative decay of the triplet states in solution is efficient, which is the reason why long-lived emission cannot be observed in solution, but the intensity and lifetime of the prompt fluorescence decrease significantly in the presence of air.

The ratios between air-equilibrated and degassed toluene solutions of Φ_{PL} (2.43) and lifetime (2.41) for **TCA_C4** are identical (**Figures S4-S6**), thus clearly the radiative rate constant of the singlet state remains unchanged. Also, the prompt fluorescence spectra do not change with time delay regardless of the presence of oxygen (**Figure S10**), thus suggesting that both quenched and unquenched emission originates from only one excited state which is also confirmed by the mono-exponential decay of the **TCA_C4** prompt fluorescence both with and without oxygen. (**Figure S5**). The large photoluminescence oxygen quenching effect, of *ca.* 2.4 in toluene, can be explained solely by quenching of the prompt fluorescence and not TADF. Again, this can be attributed to the strong mixed character of the optical transitions.

Prompt fluorescence (PF) observed in zeonex films (**Figure 2 d**) has the same spectral shape as the emission in cyclohexane (**Figure 2 a**). That means no excimers nor aggregates are formed in the solid state. In both cases (**TCA_C4**, **ThTCA_C12**) the delayed fluorescence spectra are identical to the prompt fluorescence spectra at room temperature (**Figure 2 d** and **Figure S19 b**). At 80K and long times >1 ms clear phosphorescence, from T_1, is observed (**Figure 2 d**). From this, the **TCA_C4** S_1-T_1 gap is calculated, 0.21 eV.

The small ΔE_{ST} for a non-ICT molecule observed in **TCA_C4** and its derivatives must derive from the structural geometry of the molecule. While a planar geometry is known to lower triplet energy, distorting the molecule rises it significantly.[28,29] Propeller-shaped **TCA_C4** has sufficient conjugation throughout the molecule to make the singlet state delocalised and hence low energy, while its non-planar propeller structure increases (relatively) the triplet energy. These two effects result in the observed small ΔE_{ST}. A consequence of this structure is seen in a differential redshift of the triplet energy with respect to the singlet in mCP film (SI **Figure S11**). This we ascribe to molecular compression by the dense rigid mCP matrix which flattens the

molecular conformation slightly, which in turn increases the electron exchange energy but affects the singlet state less. This is a novel observation, due to the propeller geometry of **TCA_C4.**

To investigate the photophysical properties of **TCA_C4** further, time-resolved photoluminescence measurements were made. The existence of two components in the photoluminescence emission at 300K (**Figure 2 b** and **S11-12**) can be observed in zeonex. A prompt fluorescence and a second, long-lived component having the same spectral shape, which is delayed fluorescence, which is clearly temperature-dependent. The delayed fluorescence component contributes ≈ 30% of the total emission in zeonex and mCP (see **Table S2**) which is much larger than in Hatakeyama's et al.[16] molecules (≈ 5%). At 80K, no delayed fluorescence is observed in either molecule, whereas phosphorescence (τ_{phos} = 250 ± 25 ms in **TCA_C4** and τ_{phos} = 92 ± 15 ms in **ThTCA_C12**) is clearly observed (**Figures S7 b** and **S20 b**). It can be noted that the delayed fluorescence component of **ThTCA_C12** has a longer lifetime (τ_{DF} = 3.5 ± 0.9 ms), **Figure S20 a**, than the bi-exponential emission in **TCA_C4** (τ_{DF1} = 2.1 ± 0.5 ms and τ_{DF2} = 0.6 ± 0.2 ms), **Figure S7 a**, which we ascribe to the larger singlet-triplet energy splitting of **ThTCA_C12** (**Figure S19 b**). It is noteworthy that the long triplet lifetime (low phosphorescent decay rate) is one of the principal reasons that TADF is observed in these systems as it allows time for rIC and rISC to occur from the triplet state before the triplets can decay radiatively or non-radiatively.[30]

The temperature dependence of DF in these systems is clearly observed (**Figure 2 c** and **Figure S19 c**) and follows an Arrhenius relationship. The activation energy (E_a) of the materials (0.12 eV in **TCA_C4** and 0.19 eV in **ThTCA_C12**) follows the same trend as with the magnitude of ΔE_{ST} and also like most ICT materials $E_a < \Delta E_{ST}$.[4] The DF turn-on temperature for

ThTCA_C12 (200K) is slightly higher than for **TCA_C4** (180K) (**Figure S19 c** and **Figure 2 c**). The triplet state of **ThTCA_C12** being lower in energy and having a larger ΔE_{ST} has greatly reduced rIC and no triplet state is energetically in resonance with S_1. **Figure S13** and **S19 d** confirm the intramolecular origin of delayed fluorescence (TADF) in **TCA_C4** and **ThTCA_C12** due to the linear dependence on excitation power, which rules out triplet-triplet annihilation as the route of the DF.[4,31–33]

The differences observed between the solution and solid state and the lack of influence of solution polarity on the fluorescence spectrum and lifetime with changing environment, show **TCA_C4** behaves very differently to ICT TADF molecules.[4,32,34]

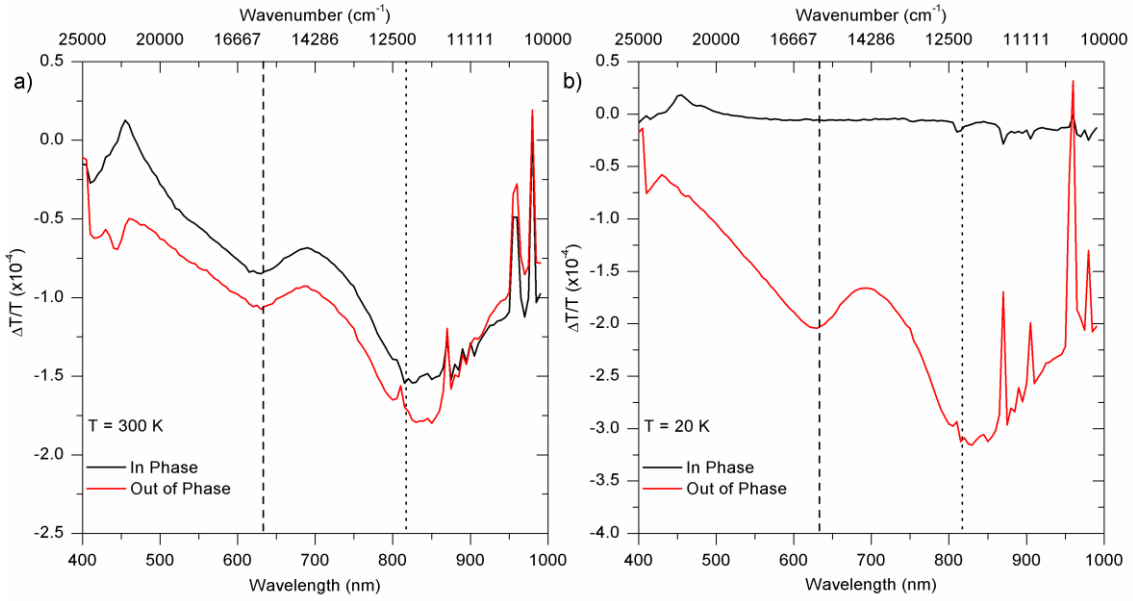

Figure 3. Quasi-steady state photoinduced absorption of **TCA_C4** in zeonex at 1% weight doping. a) The spectra measured at room temperature showing that there are contributions to the signal both at short (in phase) and long (out of phase) timescales. b) The spectra measured at 20 K showing that the in-phase contribution has disappeared thus leaving a long-lived, out of phase component only.

To further investigate the behaviour of the dark triplet states in **TCA_C4**, quasi-steady state photoinduced absorption (PIA) of **TCA_C4** is shown in **Figure 3**. The PIA of **TCA_C4** shows two bands, one at 1.96 eV (15789 cm^{-1}, 633 nm), and a second at 1.52 eV (12239 cm^{-1}, 817 nm). These two transitions are ascribed from T_1 up to high energy triplet excited states (T_n, T_m *not* T_2 or T_3). In the literature, the PIA of triphenylamine (TPA) is given showing a characteristic feature at 2.36 eV (19050 cm^{-1}) observed (in 3-methylpentane solution).[35] Further, whilst not quoted numerically in the original literature work, there is a shoulder on the PIA of TPA at 1.92 eV (15500 cm^{-1}). Thus, there is a 0.4 eV energy shift between the induced bands in **TCA_C4** and TPA.[29,36] The calculations (see SI, section 7) have shown the T_1 is mostly located on the TPA unit of **TCA_C4**, implying that **TCA_C4** has a TPA-like triplet having extended conjugation into its phenyl arms which supports this argument of a general 0.4 eV red shift of all triplet features.

Considering the phase and the temperature dependence of the PIA. We need to understand that the PIA spectra give a measure of the difference in sample absorption with the excitation light on and off and depends on the lifetime of the excited state population created by the excitation. An in-phase signal shows a population that is present on the timescale of the reference lock-in signal, in this case the sample fluorescence. Out-of-phase signals arise therefore from populations that are present at much longer times compared to the fluorescence. The 73 Hz excitation laser modulation frequency sets up the timescale of the experiment in the ≈ 10 ms region, given that the in-phase and out-of-phase spectra are recorded few milliseconds apart by average. From **Figure 3a**, the PIA measured at 300 K shows the in-phase signal that has fluorescence, +ve ΔT/T signal (450 nm), and the two characteristic induced absorption bands of

the (shifted) TPA triplet states, -ve ΔT/T signals. In the out-of-phase signal the fluorescence is no longer observed but the triplet bands are observed with stronger intensity. At 20 K, **Figure 3b**, only fluorescence is observed in the in-phase spectrum whereas only the triplet PIA is observed in the out-of-phase spectrum.

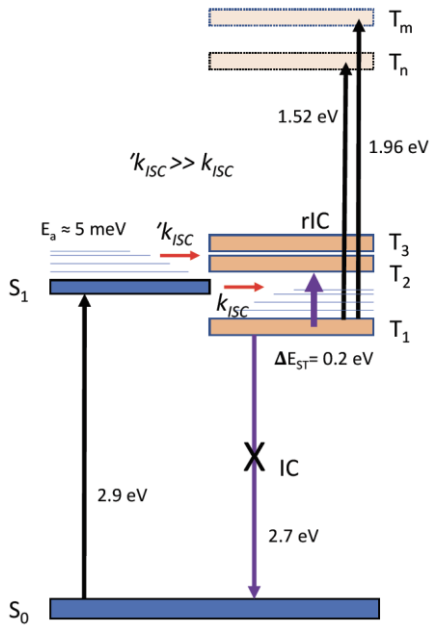

Figure 4. Schematic of the energy levels involved in the photoinduced measurements. The thermal activation barrier, E_a for ISC between S_1 and T_2/T_3 is estimated from the temperature dependence of the in-phase PIA signal. At 20 K, IC from T_1 to S_0 is assumed to be negligible.

These spectra mean that there is a triplet population created rapidly at room temperature, on a timescale faster than fluorescence which then gives rise to the delayed fluorescence, whereas at 20 K there is only much slower triplet population build up. Note, direct kinetics cannot be derived from these quasi steady state measurements. These observations can be explained by two competing ISC channels, see **Figure 4**. The first is thermally activated between S_1 and T_2/T_3. As

this is ISC between different orbital geometries the spin orbit coupling (SOC) will be efficient and the very small activation energy (estimated at 5-10 meV) gives rise to rapid ISC, on a similar timescale to the S_1 radiatve decay, $'k_{ISC} \sim 1\times10^7$ s^{-1}. IC from T_2/T_3 to T_1 is fast creating the rapid T_1 population. As this channel is thermally-activated rIC is not active at 20 K. The second channel is a slow ISC between S_1 and T_1. This is much slower as the orbitals of S_1 and T_1 are the same reducing the SOC rate and the energy gap between them is 0.2 eV. At 20 K this channel builds up a smaller triplet population in T_1, but also at 20K the triplet lifetime becomes very long (IC to S_0 negligible) and so PIA from T_1 to T_n and T_m is still strongly observed.

In all media, except zeonex, we observe the loss of a (vibronic) contribution on the blue edge of the steady-state emission spectrum at 80 K compared to room temperature. This we ascribe to the loss of a hot emission band from a vibronically excited S_1 state (see SI **Figure S14**), in the rigid molecule (in a rigid environment) and is consistent with the model we propose to explain the temperature dependence of the PIA. In zeonex, there is always free void allowing the molecule to structurally relax at all temperatures and presumably vibrationally cool. This is an important factor to consider for all molecules having thermally activated behaviour, they may retain vibrational energy for a long time compared to normal 100 fs vibrational cooling [37] when conformationally restrained in a rigid matrix environment.

Throughout our measurements, the DF component is always found to have a linear dependence on excitation power as expected for a monomolecular rISC process. At 80 K when rICDF is inactive, only phosphorescence is observed, **Figure S15 and S16**, however at very high excitation powers in mCP we do see onset of a small DF signal along with phosphorescence which we ascribe to weak TTA. From this we conclude that rICDF totally out competes TTA once enough thermal energy is available to initiate the rIC step. We also confirm that none of the

DF in guest host systems arises from possible dimer states, as in neat **TCA_C4** at room temperature a clear dimer emission is observed below the phosphorescence energy and at intermediate times, **Figure S17**, confirming that such species are not seen in dilute guest host.

The mechanism of rICDF we proposed for **TCA_C4** is supported by our previous findings in simple aromatic carbonyls.[38] In these latter materials it was found that fast S_1-T_2 ISC was mediated by the change in orbital character between the $^1\pi\pi^*$ S_1 and $^3n\pi^*$ T_2 upper triplet state leading to a DF contribution. In this case the equilibrium between S_1 and T_2 lasted hundreds of ns to yield a sub μs DF contribution but no long lived DF signal commensurate with rIC as the T_1-T_2 gap was too large in this case. However, the results clearly demonstrate that rISC from upper triplet states to S_1 can be fast, allowing for efficient rISC and TADF. With **TCA_C4** the small T_1 T_2/T_3 gap enhances this by also allowing efficient rIC. Northey and Penfold[39] have published a theoretical exploration of TADF in the nitrogen-boron compound described by Hatakeyama *et al.*[16] They find that again DF arises through upper triplet state crossing and that a thermal equilibration between T_1 and T_2 exists as the energy gap between the two is of order 0.15 eV. However, in this case they find that the ISC rate from T_2 to S_1 is slow but accelerated by S_1 state vibronic coupling to higher lying singlet states having stronger SOC to the triplet manifold. This identifies the clear need for efficient SOC between the S_1 and upper (resonant) triplet states to yield fast ISC and rISC. Clearly **TCA_C4** shows a much greater DF contribution than Hatakeyama *et al's* material because the ISC/rISC rate between S_1 and T_2/T_3 is much faster which we have ascribed to the difference in orbital geometries between the states that facilitate strong SOC.

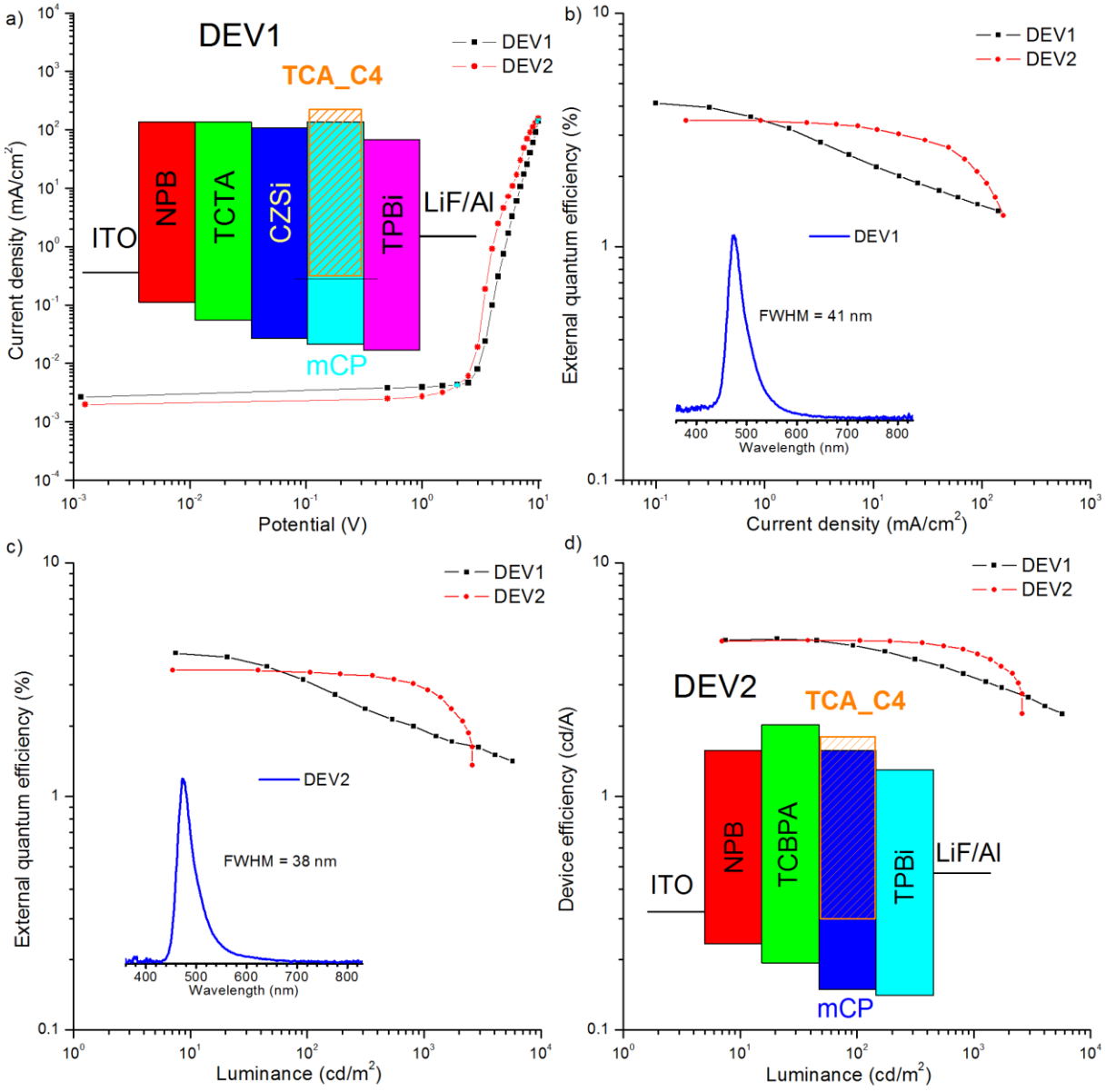

Figure 5. The comparison of the different structures of **TCA_C4** based OLED devices: Current density vs. bias (a). EQE vs current density (b), EQE vs. luminance (c), device efficiency vs. luminance (d), insets in figures a) and d) are the device structures, while insets in figures b) and c) are electroluminescence spectra.

To demonstrate the potential for **TCA_C4** to harvest triplets by this mechanism**,** OLED devices were fabricated (**Figure 5**), details given in the supplementary information (in section 3). The two device architectures compared were ITO/NPB (30 nm)/TCBPA(10 nm)/10 wt% **TCA_C4** in mCP (20 nm)/TPBi (50 nm)/LiF (1 nm)/Al (100 nm)-DEV1 and ITO/NPB (30 nm)/TCTA (15 nm)/CzSi (10 nm)/10 wt% **TCA_C4** in mCP (20 nm)/TPBi (50 nm)/LiF (1 nm)/Al (100 nm)-DEV2. The characteristics of the dopant-host OLED structures (**Figure 5**) revealed that high efficiencies (the maximum EQE about 4.1%) were obtained for the structure with an additional CzSi layer (DEV1) but due to roll-off, at higher luminance the DEV2 structure has better efficiency (**Figure 5b**). The maximum luminance was obtained for DEV1 at around 6000 cd/m^2 whereas DEV2 achieved only half that value (**Figure 5c**). The device efficiency was similar for both structures at around 4.7 cd/A (**Figure 5d**). Very narrow (FWHM = 38 nm) electroluminescence in the sky-blue region shows that this newly discovered family of TADF emitters presents a potential to produce efficient, bright TADF OLEDs with narrow emission line widths. Such a narrow electroluminescence spectrum is particularly important for OLED displays, especially in the blue.

As **TCA_C4** is an efficient luminescent emitter, the relatively low EQE of the OLED devices is attributed to the fact that this molecule is a pure donor and as such has strong electron-blocking properties meaning injection of electrons into **TCA_C** is very difficult, as seen in the energy level schemes of the devices, **Figure 5 a**,**d** (insets). Because of this it has not been possible to access the full enhancement of triplet harvesting in these devices.

CONCLUSIONS

A new family of TADF emitters has been presented showing a new TADF mechanism by which triplet states are up-converted and cross back to the singlet manifold, driven by reverse internal conversion. Remarkably narrow electroluminescence spectra, with FWHM = 38 nm are achieved because of the non-CT nature of the excited states of these molecules. A strongly mixed nπ HOMO with electron lone pairs coming from the TPA unit, combined with the propeller shape of the carbazole units leads to a small HOMO-LUMO overlap as the LUMO has π^* character. The overlap-forbidden nature of an $n\pi^*$ transition, the delocalization of the singlet state via conjugation, and the structural geometry that localizes the triplet orbitals, here has the same effect on the molecule as the CT transition or metal-ligand charge transfer (MLCT) transition in metalorganic complexes, therefore a concept of non-CT TADF molecules can be developed. Furthermore, as the HOMO has the strongly mixed nπ character the optical transitions retain high oscillator strength and exhibit high PLQY. This new combination of physicochemical properties of a non-CT molecule yield TADF by a different physical mechanism predominantly controlled by reverse internal conversion, rICDF. We show using photoinduced absorption that ISC from S_1 to T_2/T_3 is thermally activated with a small activation energy but high SOC efficiency. However, this then translates into a very high rISC rate so that the rICDF is dominated by the rIC step. Due to the pure donor (this work) or pure acceptor[17] properties of the non-CT TADF emitters, the fabrication of an efficient device may be a serious challenge. However, the non-CT molecules with a small ΔE_{ST} may be successfully applied to exciplex OLEDs as donors or acceptors. The molecule reported by Li et al.[17] was successfully applied as an exciplex device increasing EQE to 11.3% maximum.[40] Donor-acceptor ICT compounds are just one of the ways to achieve small HOMO – LUMO overlap and therefore small ΔE_{ST}. In this

work, a molecule that clearly does not contain any D-A structure has been presented that also shows TADF. There are likely many more already published molecules with unrecognized TADF properties.

ASSOCIATED CONTENT

Supporting Information.

Details of experimental methods, calculations and supporting photophysical data (PDF)

AUTHOR INFORMATION

Notes

The authors declare no competing financial interests.

ACKNOWLEDGMENT

This work was funded in part by a research grant no. 2012/05/B/ST5/00745 from National Science Centre, Poland. P.P. acknowledges the EU's Horizon 2020 for funding the EXCILIGHT project under grant agreement No 674990. P.D. acknowledges the EU's Horizon 2020 for funding the H2020-MSCA-IF-2014/659288 project "TADFORCE". M.K.E. acknowledges the EU's Horizon 2020 for funding the PHEBE project under grant agreement No. 641725.

REFERENCES

1 Endo, A.; Ogasawara, M.; Takahashi, A.; Yokoyama, D.; Kato, Y.; Adachi, C. Thermally Activated Delayed Fluorescence from Sn4+-Porphyrin Complexes and Their Application to Organic Light Emitting Diodes - A Novel Mechanism for Electroluminescence. *Adv. Mater.* **2009**, *21*, 4802–4806.

2 Tao, Y.; Yuan, K.; Chen, T.; Xu, P.; Li, H.; Chen, R.; Zheng, C.; Zhang, L.; Huang, W. Thermally Activated Delayed Fluorescence Materials Towards the Breakthrough of Organoelectronics. *Adv. Mater.* **2014**, *26*, 7931–7958.

3 Nasu, K.; Nakagawa, T.; Nomura, H.; Lin, C.-J.; Cheng, C.-H.; Tseng, M.-R.; Yasuda, T.; Adachi, C. A Highly Luminescent Spiro-Anthracenone-Based Organic Light-Emitting Diode Exhibiting Thermally Activated Delayed Fluorescence. *Chem. Commun.* **2013**, *49*, 10385.

4 Dias, F. B.; Bourdakos, K. N.; Jankus, V.; Moss, K. C.; Kamtekar, K. T.; Bhalla, V.; Santos, J.; Bryce, M. R.; Monkman, A. P. Triplet Harvesting with 100% Efficiency by Way of Thermally Activated Delayed Fluorescence in Charge Transfer OLED Emitters. *Adv. Mater.* **2013**, *25*, 3707–3714.

5 Uoyama, H.; Goushi, K.; Shizu, K.; Nomura, H.; Adachi, C. Highly Efficient Organic Light-Emitting Diodes from Delayed Fluorescence. *Nature* **2012**, *492*, 234–238.

6 Lee, D. R.; Kim, M.; Jeon, S. K.; Hwang, S.; Lee, C. W.; Lee, J. Y. Design Strategy for 25% External Quantum Efficiency in Green and Blue Thermally Activated Delayed Fluorescent Devices. *Adv. Mater.* **2015**, *27*, 5861–5867.

7 Cho, Y. J.; Chin, B. D.; Jeon, S. K.; Lee, J. Y. 20% External Quantum Efficiency in Solution-Processed Blue Thermally Activated Delayed Fluorescent Devices. *Adv. Funct. Mater.* **2015**, *25*, 6786–6792.

8 Higginbotham, H.; Karon, K.; Ledwon, P.; Data, P. Carbazoles in Optoelectronic Applications. *Disp. Imaging* **2017**, *2*, 207–216.

9 Jankus, V.; Data, P.; Graves, D.; McGuinness, C.; Santos, J.; Bryce, M. R.; Dias, F. B.; Monkman, A. P. Highly Efficient TADF OLEDs: How the Emitter-Host Interaction Controls Both the Excited State Species and Electrical Properties of the Devices to Achieve Near 100% Triplet Harvesting and High Efficiency. *Adv. Funct. Mater.* **2014**, *24*, 6178–6186.

10 Data, P.; Kurowska, A.; Pluczyk, S.; Zassowski, P.; Pander, P.; Jedrysiak, R.; Czwartosz, M.; Otulakowski, L.; Suwinski, J.; Lapkowski, M.; Monkman, A. P. Exciplex Enhancement as a Tool to Increase OLED Device Efficiency. *J. Phys. Chem. C* **2016**, *120*, 2070–2078.

11 Data, P.; Motyka, R.; Lapkowski, M.; Suwinski, J.; Jursenas, S.; Kreiza, G.; Miasojedovas, A.; Monkman, A. P. Efficient P-Phenylene Based OLEDs with Mixed Interfacial Exciplex Emission. *Electrochim. Acta* **2015**, *182*, 524–528.

12 Zhang, T.; Chu, B.; Li, W.; Su, Z.; Peng, Q. M.; Zhao, B.; Luo, Y.; Jin, F.; Yan, X.; Gao, Y.; Wu, H.; Zhang, F.; Fan, D.; Wang, J. Efficient Triplet Application in Exciplex Delayed-Fluorescence OLEDs Using a Reverse Intersystem Crossing Mechanism Based on a Δ E S–T of around Zero. *ACS Appl. Mater. Interfaces* **2014**, *6*, 11907–11914.

13 Lee, I. H.; Song, W.; Lee, J. Y. Aggregation-Induced Emission Type Thermally Activated Delayed Fluorescent Materials for High Efficiency in Non-Doped Organic Light-Emitting Diodes. *Org. Electron.* **2016**, *29*, 22–26.

14 Nikolaenko, A. E.; Cass, M.; Bourcet, F.; Mohamad, D.; Roberts, M. Thermally Activated Delayed Fluorescence in Polymers: A New Route toward Highly Efficient Solution Processable OLEDs. *Adv. Mater.* **2015**, *27*, 7236–7240.

15 Nobuyasu, R. S.; Ren, Z.; Griffiths, G. C.; Batsanov, A. S.; Data, P.; Yan, S.; Monkman, A. P.; Bryce, M. R.; Dias, F. B. Rational Design of TADF Polymers Using a Donor-Acceptor Monomer with Enhanced TADF Efficiency Induced by the Energy Alignment of Charge Transfer and Local Triplet Excited States. *Adv. Opt. Mater.* **2016**, *4*, 597–607.

16 Hatakeyama, T.; Shiren, K.; Nakajima, K.; Nomura, S.; Nakatsuka, S.; Kinoshita, K.; Ni, J.; Ono, Y.; Ikuta, T. Ultrapure Blue Thermally Activated Delayed Fluorescence Molecules: Efficient HOMO-LUMO Separation by the Multiple Resonance Effect. *Adv. Mater.* **2016**, *28*, 2777–2781.

17 Li, J.; Zhang, Q.; Nomura, H.; Miyazaki, H.; Adachi, C. Thermally Activated Delayed Fluorescence from 3nπ * to 1nπ * up-Conversion and Its Application to Organic Light-Emitting Diodes. *Appl. Phys. Lett.* **2014**, *105*, 13301.

18 Mamada, M.; Inada, K.; Komino, T.; Potscavage, W. J.; Nakanotani, H.; Adachi, C. Highly Efficient Thermally Activated Delayed Fluorescence from an Excited-State Intramolecular Proton Transfer System. *ACS Cent. Sci.* **2017**, *3*, 769–777.

19 Lim, B. T.; Okajima, S.; Chandra, A. K.; Lim, E. C. Radiationless Transitions in Electron Donor–acceptor Complexes: Position-dependent Deuterium Isotope Effects on S1 → S0 Internal Conversion of 1:1 and 2:1 Complexes of Methyl-substituted Benzenes with Tetracyanobenzene. *J. Chem. Phys.* **1982**, *77*, 3902–3909.

20 Dias, F. B.; Santos, J.; Graves, D. R.; Data, P.; Nobuyasu, R. S.; Fox, M. A.; Batsanov, A. S.; Palmeira, T.; Berberan-Santos, M. N.; Bryce, M. R.; Monkman, A. P. The Role of Local Triplet Excited States and D-A Relative Orientation in Thermally Activated Delayed Fluorescence: Photophysics and Devices. *Adv. Sci.* **2016**, *3*, 1600080.

21 Etherington, M. K.; Gibson, J.; Higginbotham, H. F.; Penfold, T. J.; Monkman, A. P. Revealing the Spin–vibronic Coupling Mechanism of Thermally Activated Delayed Fluorescence. *Nat. Commun.* **2016**, *7*, 13680.

22 Gibson, J.; Monkman, A. P.; Penfold, T. J. The Importance of Vibronic Coupling for Efficient Reverse Intersystem Crossing in Thermally Activated Delayed Fluorescence Molecules. *ChemPhysChem* **2016**, *17*, 2956–2961.

23 Samsung demonstrate a healthier Bio-Blue OLED display at SID 2016 https://www.oled-info.com/samsung-demonstrate-healthier-bio-blue-oled-display-sid-2016 (accessed Nov 1, 2017).

24 Cherpak, V.; Stakhira, P.; Minaev, B.; Baryshnikov, G.; Stromylo, E.; Helzhynskyy, I.; Chapran, M.; Volyniuk, D.; Hotra, Z.; Dabuliene, A.; Tomkeviciene, A.; Voznyak, L.; Grazulevicius, J. V. Mixing of Phosphorescent and Exciplex Emission in Efficient Organic Electroluminescent Devices. *ACS Appl. Mater. Interfaces* **2015**, *7*, 1219–1225.

25 Chakravorty, K.; Poole, J. A. The Effect of Dissolved Molecular Oxygen on the Fluorescence of 9,10-Diphenylanthracene. *J. Photochem.* **1984**, *26*, 25–31.

26 Cox, M. E.; Dunn, B. Detection of Oxygen by Fluorescence Quenching. *Appl. Opt.* **1985**, *24*, 2114-2120.

27 Wilkinson, F.; McGarvey, D. J.; Olea, A. F. Excited Triplet State Interactions with Molecular Oxygen: Influence of Charge Transfer on the Bimolecular Quenchfng Rate Constants and the Yields of Singlet Oxygen (O2,1Δg) for Substituted Naphthalenes in Various Solvents. *J. Phys. Chem.* **1994**, *98*, 3762–3769.

28 Strohriegl, P.; Wagner, D.; Schrögel, P.; Hoffmann, S. T.; Köhler, A.; Heinemeyer, U.; Münster, I. Novel Host Materials for Blue Phosphorescent OLEDs. In *Proceedings of SPIE*; So, F., Adachi, C., Eds.; 2013; Vol. 8829, p 882906; SPIE: Bellingham, United States, 2013.

29 Bagnich, S. A.; Athanasopoulos, S.; Rudnick, A.; Schroegel, P.; Bauer, I.; Greenham, N. C.; Strohriegl, P.; Köhler, A. Excimer Formation by Steric Twisting in Carbazole and Triphenylamine-Based Host Materials. *J. Phys. Chem. C* **2015**, *119*, 2380–2387.

30 Pander, P. H.; Swist, A.; Soloducho, J.; Dias, F.; Data, P. Thermally Activated Delayed Fluorescence with Narrow Emission Spectrum and Organic Room Temperature Phosphorescence by Controlling Spin-Orbit Coupling and Phosphorescence Lifetime of Metal-Free Organic Molecules. *J. Mater. Chem. C* **2018**, *6*, 5434–5443.

31 Jankus, V.; Chiang, C. J.; Dias, F.; Monkman, A. P. Deep Blue Exciplex Organic Light-Emitting Diodes with Enhanced Efficiency; P-Type or E-Type Triplet Conversion to Singlet Excitons? *Adv. Mater.* **2013**, *25*, 1455–1459.

32 Data, P.; Pander, P.; Okazaki, M.; Takeda, Y.; Minakata, S.; Monkman, A. P. Dibenzo[a,j]Phenazine-Cored Donor-Acceptor-Donor Compounds as Green-to-Red/NIR Thermally Activated Delayed Fluorescence Organic Light Emitters. *Angew. Chemie Int. Ed.* **2016**, *55*, 5739–5744.

33 Dos Santos, P. L.; Dias, F. B.; Monkman, A. P. Investigation of the Mechanisms Giving Rise to TADF in Exciplex States. *J. Phys. Chem. C* **2016**, *120*, 18259–18267.

34 dos Santos, P. L.; Ward, J. S.; Bryce, M. R.; Monkman, A. P. Using Guest–Host

Interactions To Optimize the Efficiency of TADF OLEDs. *J. Phys. Chem. Lett.* **2016**, *7*, 3341–3346.

35 Henry, B. R.; Kasha, M. Triplet-Triplet Absorption Studies on Aromatic and Heterocyclic Molecules at 77 K. *J. Chem. Phys.* **1967**, *47*, 3319–3326.

36 Huang, S.; Zhang, Q.; Shiota, Y.; Nakagawa, T.; Kuwabara, K.; Yoshizawa, K.; Adachi, C. Computational Prediction for Singlet- and Triplet-Transition Energies of Charge-Transfer Compounds. *J. Chem. Theory Comput.* **2013**, *9*, 3872–3877.

37 Dai, D. C.; Monkman, A. P. Femtosecond Hot-Exciton Emission in a Ladder-Type π-Conjugated Rigid-Polymer Nanowire. *Phys. Rev. B* **2013**, *87*, 45308.

38 Torres Ziegenbein, C.; Fröbel, S.; Glöß, M.; Nobuyasu, R. S.; Data, P.; Monkman, A.; Gilch, P. Triplet Harvesting with a Simple Aromatic Carbonyl. *ChemPhysChem* **2017**, *18*, 2305–2305.

39 Northey, T.; Penfold, T. J. The Intersystem Crossing Mechanism of an Ultrapure Blue Organoboron Emitter. *Org. Electron.* **2018**, *59*, 45–48.

40 Li, J.; Nomura, H.; Miyazaki, H.; Adachi, C. Highly Efficient Exciplex Organic Light-Emitting Diodes Incorporating a Heptazine Derivative as an Electron Acceptor. *Chem. Commun.* **2014**, *50*, 6174–6176.

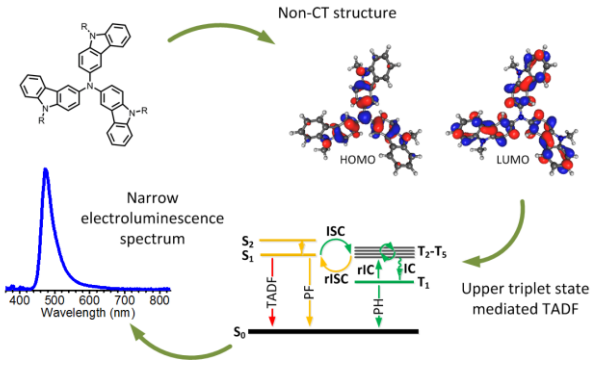
Non-CT structure
HOMO
LUMO
Upper triplet state
mediated TADF
ISC
rISC
rIC
IC
TADF
PF
PH
Narrow
electroluminescence
spectrum
400 500 600 700 800
Wavelength (nm)